Stability and nuclear formation of Si(111)-7 × 7 structure as determined from charge redistribution in surface layers

Koji Miyake [a],[*],[1], Haruhiro Oigawa [a], Kenji Hata [a], Ryuji Morita [b], Mikio Yamashita [b], Hidemi Shigekawa [a],[c]

[a] *Institute of Applied Physics, and Center for TARA, Tsukuba Advanced Research Alliance, CREST,
Japan Science and Technology Corporation (JST), University of Tsukuba, Tsukuba 305-8573, Japan*
[b] *Department of Applied Physics, CREST, Japan Science and Technology Corporation (JST), Hokkaido University,
Sapporo 060-8628, Japan*
[c] *Department of Chemistry and Biotechnology, Graduate School of Engineering, The University of Tokyo, Hongo,
Tokyo 113-8656, Japan*

Abstract

By considering the charge transfer from adatoms to rest atoms, the structure of the dimer and stacking-fault (DS) layers in the Si(111) dimer–adatom–stacking-fault (DAS) structure was analyzed at a subunit level on a quenched surface. In comparison with the modified model of Vanderbilt, corner holes with a completed DS structure in the second layer, completed corner holes, were confirmed to play a key role not only in the mechanism to stabilize the DAS structure, but also in its formation process. The formation of the completed corner hole works as a rate-limiting process for the growth of the DAS structure. This mechanism was shown to be quite consistent with the experimental results obtained using scanning tunneling microscopy on the quenched Si(111) surface. © 1999 Elsevier Science B.V. All rights reserved.

1. Introduction

The reconstruction of the Si(111) surface has been extensively studied by various experiments and theoretical considerations [1–5], and the 7 × 7 structure has been concluded to be the most stable phase on the Si(111) surface in equilibrium condition. In fact, the 7 × 7 phase is completed on the well-annealed surface, and a phase transition between high-temperature '1 × 1' and 7 × 7 phases was directly observed around the critical temperature by using scanning tunneling microscopy (STM) [6,7]. The dimer–adatom–stacking-fault (DAS) structure proposed by Takayanagi et al. [1], which is compatible with the experimental and theoretical results, is widely accepted as the model for the Si(111)-7 × 7 reconstructed surface structure, and atomic arrangement of the DAS structure in the static form is now well established. However, since the DAS structure involves few surface layers and is very complicated, the dynamics of the surface, the mechanism for the formation and the stabilization processes of the structure have not

---

* Corresponding author.
E-mail addresses: miyake@ims.tsukuba.ac.jp (K. Miyake),
hidemi@ims.tsukuba.ac.jp (H. Shigekawa)
[1] *Internet address:* http://dora.ims.tsukuba.ac.jp

yet been completely clarified, and is still attracting considerable attention.

In the non-equilibrium Si(111) surface prepared, for example, by laser-annealing or quenching, metastable (non-7×7) phases are known to be formed on the surface: 9×9, 11×11, 2×2, $c(2 \times 4)$ and $\sqrt{3} \times \sqrt{3}$ (all of which have higher atomic densities than the 7×7), and 5×5 and 2×1, which have lower atom densities than 7×7 [8–12]. Since the stability and dynamics of the metastable structures on the surface are essential factors in understanding the mechanism of the surface reconstruction, it is very important to elucidate the structures in detail.

Recently, the dynamic growth step of $(2n+1) \times (2n+1)$ DAS structures was directly observed on a quenched Si(111) surface at ~ 750 K using STM [13]. All of the metastable $(2n+1) \times (2n+1)$ DAS domains ($n \neq 3$) that formed on the quenched surface did not survive, but transformed into the 7×7 DAS domains at the end. However, during the fluctuation, growth and annihilation of $(2n+1) \times (2n+1)$ DAS, domains were observed to occur with a single $(2n+1) \times (2n+1)$ stacking-fault (SF) half-cell as the building unit. The $(2n+1) \times (2n+1)$ DAS domains grow in a triangular shape with the successive addition of single SF half-cells to a $(2n+1) \times (2n+1)$ DAS domain side. In the growth process, SF half-cells were formed sharing corner holes.

On the other hand, Vanderbilt analyzed the energetics of the Si(111) surface, and proposed a model to explain the phase diagram on the surface [14]. Experimentally, Yang and Williams [12] measured the atomic density of the high-temperature '1×1' structure, and explained the stability of the reconstructed structures by analyzing the energy balance based on the idea of atomic conservation; the formation of each phase is governed by the atomic density around the area. This mechanism was quantified by Vanderbilt by introducing the idea of the chemical potential for Si atoms in the surface layer [15]. With this model, the stability of the 7×7 structure and the formation of the other metastable (non-7×7) phases on the Si(111) surface were explained, which was in good agreement with the experimental results. However, since the analysis was performed at the level of the DAS unit, the prediction was still very limited. For example, the mechanism to explain the growth of the DAS domains in a triangular shape has not been clarified yet. In order to understand the phase transition from the standpoint of the dynamics in more detail, it is necessary to obtain information about the stability and change in the reconstructed structures at a subunit level.

As a factor in the subunit level to stabilize the DAS structure, the role of the structure consisting of a dimer and adatom pair was pointed out first [16]. However, from the observation of the stable dimer and stacking-fault (DS) cell, the effect of the adatoms was considered to be not essential [17]. In fact, in the Vanderbilt model the effect of the adatoms is treated as an additional factor to shift the energy diagram [14]. On the other hand, the importance of the corner hole has also been pointed out recently. For example, from the analysis of the structural growth of the 7×7 structure from the step edge, Ohdomari proposed a model that the DAS structure is stabilized by the structure of the corner holes fixed with oxygen atoms [18]. Experimentally, the important role of the corner hole in stabilizing the DAS structure was recognized recently even in the breakdown process of the 7×7 structure by analyzing the HBO_2 molecular adsorption process; the structure of the corner hole was observed to be maintained along the boundaries between the 7×7 and the disordered areas [19]. In addition, various $(2n+1) \times (2n+1)$ SF half-cells were observed to grow on a quenched Si(111) surface sharing corner holes. These results suggest that corner holes play an important role not only in the mechanism to stabilize the DAS phase, but also in the formation process of the DAS structure. However, as is well known, the DAS structure has a very complicated under-layer structure consisting of dimers and stacking-faults, i.e. the DS structure. Therefore, in order to understand the mechanism, clarification is needed of the detailed structure of corner holes including the DS structure. However, STM images generally give information only about the topmost layer, and the under-layer structure has not been analyzed in detail.

In this paper, we present our recent results concerning the mechanism for the stabilization and formation processes of the DAS structure at a subunit level, i.e. the role of the corner holes with the completed DS structure in the second layer. The under-layer of the DAS structure is discussed by analyzing the bias dependence of STM images on a quenched Si(111) surface as a result of the charge transfer from adatoms to the rest atoms in a unit [20,21].

2. Experimental

Phosphorus-doped n-type Si(111) (1 Ω cm) substrates were chemically cleaned and loaded into the UHV-STM chamber. After prebaking for 1 day, samples were flashed at $\sim 1100°C$, and the formation of a clean 7×7 structure was confirmed by STM. Then, samples were heated to $\sim 1000°C$, and quenched by turning off the heating power. STM measurements were performed at room temperature using an electrochemically etched tungsten tip. All STM images shown in this paper were taken in the constant-current mode.

3. Results and discussion

3.1. Role of the corner hole in the stabilization mechanism

3.1.1. Structural analysis model and its application to the analysis of the boundary between 7×7 and disordered areas

Fig. 1a shows an STM image of a quenched Si(111) surface (sample bias voltage V_s and tunneling current I_t are −2.0 V and 0.3 nA respectively). Triangular areas with disordered structure are surrounded by the 7×7 structure, as shown in the figure. Fig. 1b shows a magnified image along the straight part of the boundary between the 7×7 and disordered structural areas. There exist adatoms along the outside edge of the 7×7 triangular domain, and corner holes are formed along the boundary, as previously pointed out [19,21,22]. This structure can be seen commonly. For example, see fig. 5(c) in Ref. [23]. As a subunit factor, the
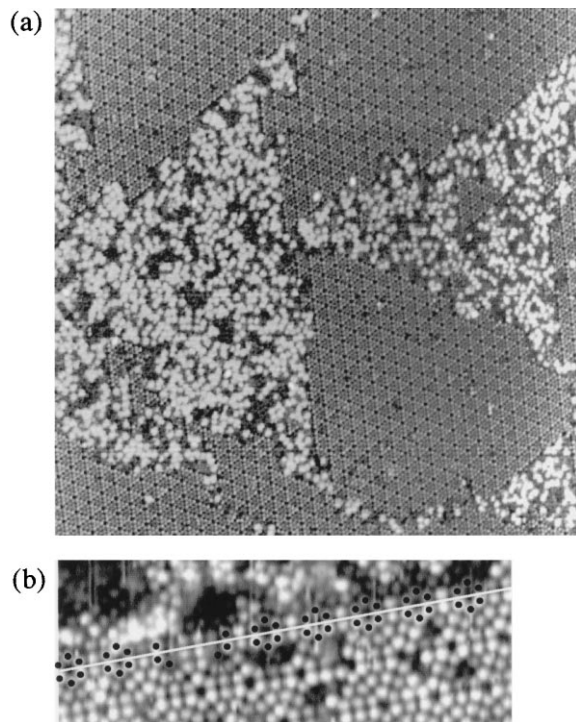

Fig. 1. (a) STM image of a quenched Si(111) surface ($V_s = -2.0$ V, $I_t = 0.3$ nA), and (b) a magnification of a boundary between the 7×7 and disordered areas.

structure of the corner hole has been pointed out as playing an important role in stabilizing the 7×7 structure as described above. Therefore, first, let us examine the under-layer structure of the boundary between the 7×7 and disordered areas.

It is well known that the DAS structure has a characteristic electronic property: the charge transfer from the top-layer adatoms to the rest atoms in the under-layer [24,25]. Since the amount of charge transfer from adatoms to rest atoms depends on the number of rest atoms that surround the adatoms, the structure of the under-layer can be discussed by considering the charge redistribution on the adatoms caused by the charge transfer from adatoms to the rest atoms [20,21]. Fig. 2a and b schematically show two possible models, in which an SF is formed (Fig. 2a) and not formed (Fig. 2b). Under-layer dimers and SF regions are represented by closed ellipses and hatched triangles respectively. If the dimers in the second layer are formed along the boundary and around the corner
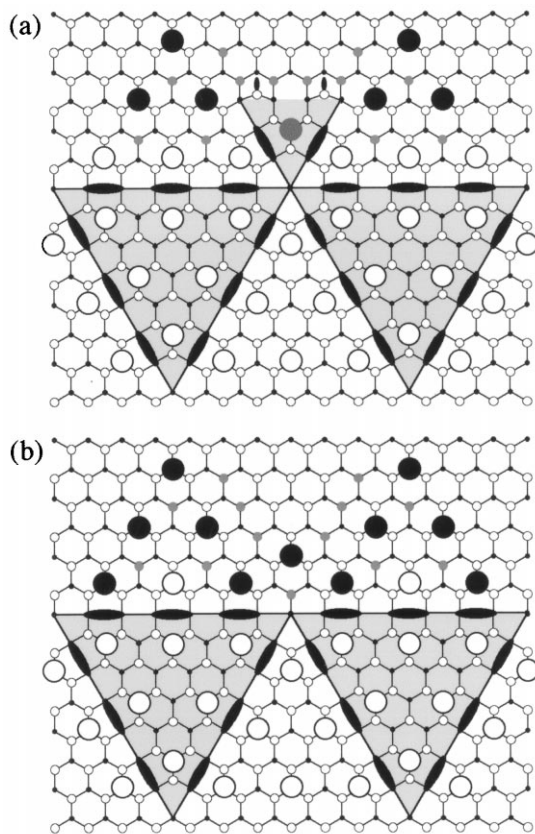
Fig. 2. Schematics of the domain boundary between the 7×7 and disordered areas, in which (a) an SF is formed and (b) not formed. Bright and dark adatoms and under-layer dimers are indicated by open and filled circles, and closed ellipses respectively.

holes through the formation of an SF as shown in Fig. 2a, the number of rest atoms around adatoms becomes the same as that in the regular 7×7 DAS structure. Therefore, the adatoms forming the corner holes and those along the boundary must be bright even in the filled-state STM image in this case. On the other hand, if an SF is not formed, as shown in Fig. 2b, charge transfer from the adatoms increases because the number of rest atoms around the adatoms increases compared with that in the regular 7×7 DAS structure. Thereby, the adatoms in the disordered area must be darker in the filled-state STM image. Normal corner and center adatoms are represented by white circles. Gray and filled circles respectively

represent those adatoms that are observed darker and those not observed in the filled state image. The difference in the brightness of the adatoms depends on the amount of charge transferred from the adatoms to the rest atoms. Normal corner and center adatoms have one and two rest atoms in their nearest neighbor sites. Adatoms that have three rest atoms in their nearest neighbor sites are not observed in the filled-state image. The number of rest atoms in the second nearest neighbor sites has an influence on the brightness of those adatoms represented by gray circles.

Let us compare the structural model described in Fig. 2 with the STM results actually obtained at a domain boundary. Fig. 3a and b shows the magnified STM images of a boundary region taken at positive and negative sample bias voltages. In the empty-state image shown in Fig. 3a ($V_s = 2.0$ V, $I_t = 0.3$ nA), it is clear that corner holes exist along the boundary between the 7×7 and disordered areas. As shown in Fig. 3b, the adatoms at the boundary and around the corner holes are bright even in the filled-state image ($V_s = -0.5$ V, $I_t = 0.3$ nA). In consideration of the charge transfer in the surface layers, these corner holes are sur-
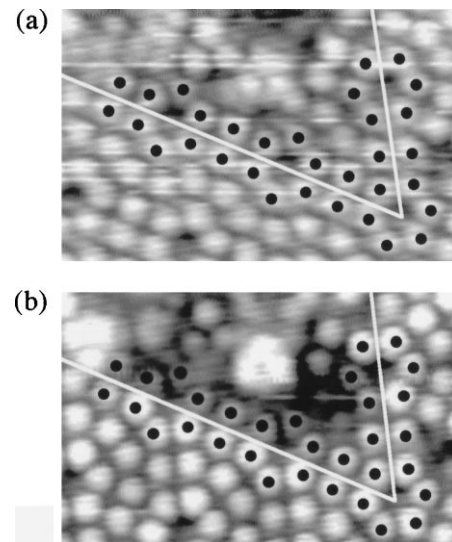

Fig. 3. Magnified images of a boundary between 7×7 and disordered areas taken at positive and negative bias voltages are shown in (a) $V_s = 2.0$ V, $I_t = 0.3$ nA and (b) $V_s = -0.5$ V, $I_t = 0.3$ nA respectively. Adatoms at the boundary are indicated by dots.

rounded by a completed SF structure, and there exist dimer chains along the outside edge of the SF units, as is shown in Fig. 2a. These results suggest that the 'completed corner hole', i.e. a corner hole with a DS structure, plays an important role in the stability of the 7×7 structure.

3.1.2. Analysis of the other DAS structures

In order to generalize the results obtained for the boundary between 7×7 and disordered areas, structures concerning the other DAS phases are examined next. Fig. 4a shows an STM image taken over a more highly quenched area ($V_s = 2.0$ V, $I_t = 0.3$ nA). As is shown in Fig. 4a, metastable phases such as 5×5, 9×9, and 11×11 structures exist in addition to the 7×7 structure. Fig. 4b shows the relative amounts of these DAS units observed on the surface. According to the model discussed by Yang and Williams [12] and Vanderbilt [15], this coexistence of DAS families is caused by a change and fluctuation in the chemical potential during the quenching. In fact, extra Si atoms are observed in the disordered area between the domains of the ordered structures. When the surface is annealed for long enough at higher temperatures, those extra Si atoms are incorporated by the steps, and the surface becomes covered by only the 7×7 phase. It was reported that the 9×9 phase with a higher atomic density grows in a fluctuation during annealing the quenched surface at a low temperature around 750 K [13], which is considered to be realized by the higher atomic density occasionally formed around the boundary due to the lower diffusion velocity of Si atoms at this temperature.

As expected, a structure similar to that observed for the 7×7 domain boundary was also observed for the other $(2n+1) \times (2n+1)$ DAS structural domain boundaries. An example observed for the 9×9 phase is shown in Fig. 5a ($V_s = 2.0$ V, $I_t = 0.3$ nA) and Fig. 5b ($V_s = -0.5$ V, $I_t = 0.3$ nA). Here, the adatoms at the boundary between the 9×9 structural domain and the disordered area are bright even in the filled-state image, indicating the existence of the DS structure in the under-layer there. The observed results suggest the existence of a general mechanism over the role of the corner hole in stabilizing the DAS structure.
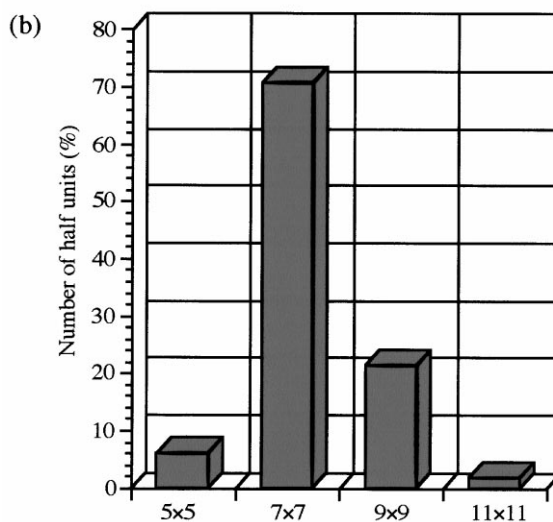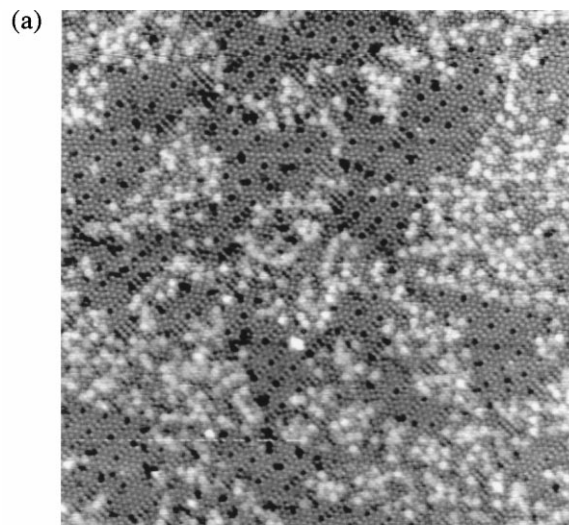

Fig. 4. (a) STM image taken over a more highly quenched surface ($V_s = 2.0$ V, $I_t = 0.3$ nA). (b) Relative amounts of DAS units observed on the surface.

3.2. Role of the corner hole in the formation process

3.2.1. Nucleation of the DAS structures

In order to elucidate the role of corner holes in more detail, we examined the structure of the DAS fragments in a disordered area. Fig. 6a and b shows empty-state ($V_s = 2.0$ V, $I_t = 0.3$ nA) and filled-state ($V_s = -0.5$ V, $I_t = 0.3$ nA) STM images. In the empty-state image (Fig. 6a), it is clearly shown that the half-unit cells of 7×7, 9×9, and
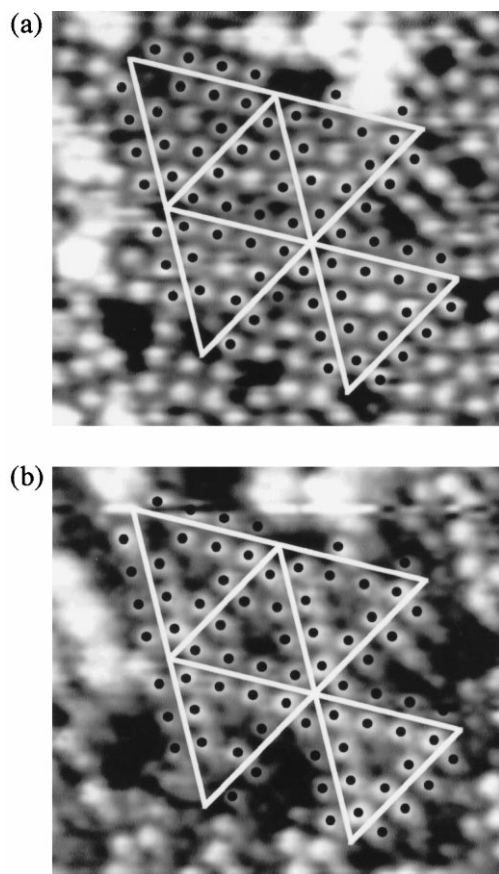
(a)

(b)

Fig. 5. STM image of a 9×9 domain structure on a quenched surface. (a) $V_s = 2.0$ V, $I_t = 0.3$ nA and (b) $V_s = -0.5$ V, $I_t = 0.3$ nA. Adatoms at the boundary are indicated by dots.

11×11 structures share the same corner hole. In addition, the adatoms existing along the boundaries of the half-unit cells are bright even in the filled-state image, as shown in Fig. 6b. Therefore, according to our structural analysis model [20,21], the DS structure must exist there. One exception is about the center adatom in the 7×7 SF unit at the boundary indicated by an arrow in Fig. 6b. The adatom looks darker in the filled-state image. However, it is brighter than the other darker adatoms in the 11×11 SF unit in Fig. 6b, and its shape is much closer to the normal center and corner adatoms. Therefore, we consider this adatom to be influenced, for example, by gas adsorption. The result obtained strongly suggests the possibility that formation of a completed

corner hole works as a nucleation center for the DAS structural formation process in the disordered area, resulting in the growth of the various $(2n+1) \times (2n+1)$ SF cells from the same corner hole. The schematic model of this structure is shown in Fig. 6c. Open, gray and filled circles indicate the adatoms with different electronic structures similar to those defined in Fig. 2.

3.2.2. Relation between 7×7 and 9×9 phases

Fig. 7 shows an STM image in which three 9×9 domains exist sharing corner holes with a 7×7 triangular domain ($V_s = -0.5$ V, $I_t = 0.3$ nA). According to the model by Yang and Williams [12] and Vanderbilt [15], the 9×9 phase is formed at a lower temperature than the 7×7 phase, due to the increase in the chemical potential induced by quenching, as described above. Therefore, 9×9 domains are considered to be formed from the corner hole on the side of the 7×7 domain, which indicates that corner holes have a key role even in the formation process, as pointed out above. In fact, during the dynamic fluctuation of the DAS structure observed by Ohdomari and coworkers on the quenched surface [13], it was generally observed that various $(2n+1) \times (2n+1)$ DAS half-cells nucleate at the side of the DAS domains sharing corner holes. Concerning the under-layer of the corner holes, since the adatoms forming corner holes are bright in the filled-state image, as shown in Fig. 7, the corner holes are completed with the DS structure. These results support the model that growth of the DAS structure is governed by the formation of the completed corner hole.

3.2.3. A model to explain the DAS formation process

On the basis of the results obtained, a possible model for the formation mechanism of the DAS structure is shown in Fig. 8, in which the formation of a completed corner hole serves as the trigger and the rate-limiting step for the 7×7 structural growth. First, a corner hole with a DS structure nucleates in the high-temperature disordered area (Fig. 8a to b). Then, SF half cells of $(2n+1) \times (2n+1)$ DAS structures grow from the corner hole (Fig. 8c). When two neighboring SF
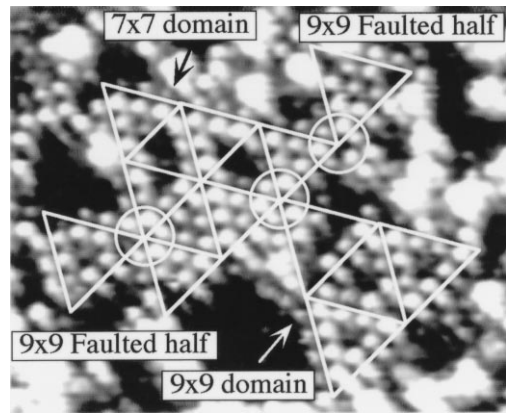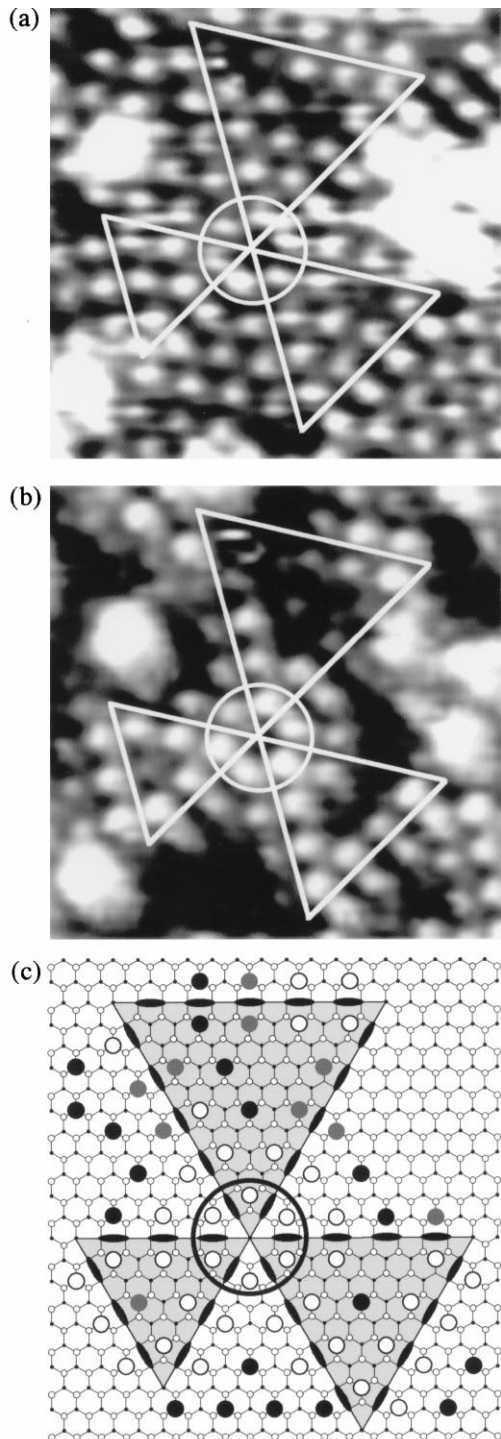
(a)

(b)

(c)

Fig. 7. STM image of a quenched Si(111) surface ($V_s = -0.5$ V, $I_t = 0.3$ nA). Three 9×9 domains exist sharing corner holes with a 7×7 triangular domain.

units have the same size, a DAS structure is formed completely by the formation of the structure of corner holes that exist on the other end of the SF unit. After formation of the corner holes, another SF cell will grow sharing the corner holes (Fig. 8d). Therefore, the growth of the 9×9 domains from the completed corner holes on the 7×7 domain sides, observed in Figs. 6 and 7, can also be explained by this model.

There exist domains consisting of single 9×9 phase; however, 9×9 domains prefer to share corner holes with 7×7 domains, as shown in Fig. 7. This result suggests the existence of a barrier height to form the completed corner hole shown in Fig. 8. On the other hand, as shown in Fig. 8, there exist three different steps in the DAS growth process: (1) nucleation process (Fig. 8a to b), (2) S-process (Fig. 8b to c) and (3) P-process (Fig. 8c to d). S- and P-processes will be explained in Section 3.4.2. Therefore, some mechanism, such as the oxygen-related process proposed by Ohdomari [18], may exist to induce the first nucleation process.

Fig. 6. Magnifications of the DAS fragments: (a) $V_s = 2.0$ V, $I_t = 0.3$ nA and (b) $V_s = -0.5$ V, $I_t = 0.3$ nA. (c) Schematic model of (b). White and gray circles indicate adatoms with normal and dark brightness in the filled-state image (b). Black circles indicate the adatoms that are bright in the empty-state image (a) but disappeared in the filled-state image (b).
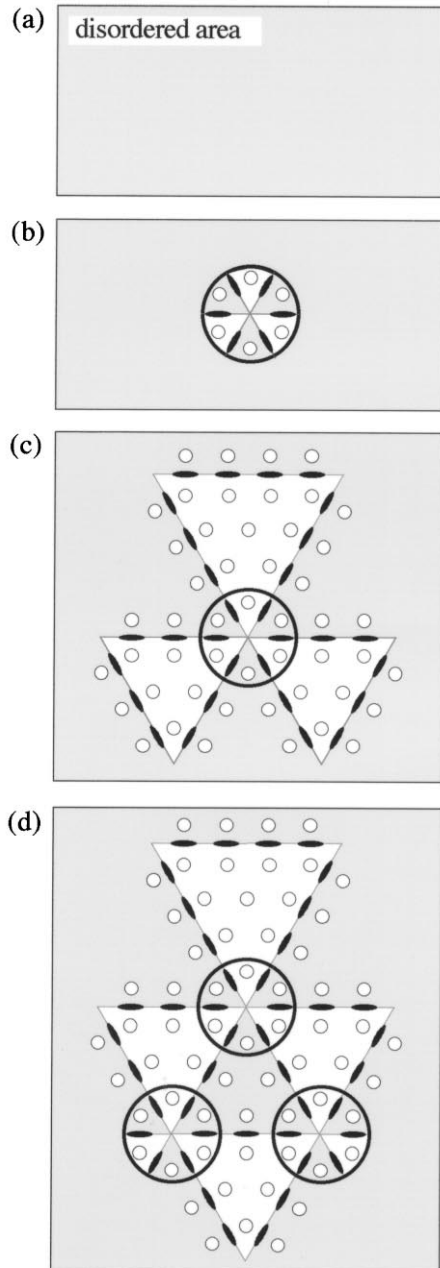
Fig. 8. Schematic diagram of the formation process of the DAS structure: (a) high-temperature disordered area, (b) nucleation of a corner hole, (c) growth of half-unit cells of DAS structures including an SF from the corner hole and (d) complete formation of the DAS structure.

3.2.4. Theoretical model based on the chemical potential

In order to examine the model proposed here, let us discuss the results observed by the theoretical model proposed by Vanderbilt [14]. As described above, following the STM work on a quenched surface by Yang and Williams [23], Vanderbilt introduced the idea of the chemical potential μ for Si atoms in the surface layer, and explained the effects of variable atomic density on the stability of the reconstructed structures [15]. Vanderbilt gave the free energy of the DAS structure per 1×1 cell relative to the 1×1 phase as [15]

$$\Delta E = \Delta f/2 + (2n\Delta w + \Delta c')/(2n+1)^2 - \mu \Delta N, \qquad (1)$$

where Δf, Δw, $\Delta c'$, and ΔN are respectively the faulting energy, the dimer wall formation energy, the normalized corner hole formation energy (including the effect of the adatom decoration), and the excess density of atoms in the surface layer per 1×1 cell relative to the simple adatom phases $\{\Delta N = -(8n+9)/[4(2n+1)^2]\}$. Substituting the values of Δf, Δw and $\Delta c'$ by 0.06 eV, -0.65 eV and 1.33 eV respectively, obtained by a combination of ab initio and empirical calculations, Eq. (1) gives the most stable phase on the Si(111) surface to be the 7×7 structure.

This model was originally derived from the analysis of the energetics among the DAS phases relative to the 1×1 structure. The comparison was based on the completed DAS units in a static form. However, the model was possibly applied to the analysis of the phase transition on a quenched surface, by introducing the idea of the chemical potential μ. From Eq. (1), the formation of the quasi-equilibrium structures (non-7×7 structures) could be explained well as a result of the fluctuation or the change in the chemical potential during the formation processes. Namely, μ is usually pinned to the bulk cohesive energy by step-mediated exchange of Si atoms. However, a supersaturated condition is apparently reached as Vanderbilt pointed out, for example, on a surface prepared by laser-annealing or quenching. In fact, various DAS phases were observed by STM on the quenched surface experimentally, indicating that

$\mu = \mu(t)$ (t: time after starting quench) for each phase was realized on the surface during the quenching.

As shown in Fig. 4b, almost 20% of the DAS structures formed on the surface in the area shown in Fig. 4a is the 9×9 phase. From Eq. (1), with an increase in $\mu = \mu(t)$ due to the change in the atomic density during quenching, the DAS structure formed on the surface changes from 7×7 to the high atomic density phase. The change in $\Delta E(n)$ of Eq. (1) for various values of the chemical potential is shown in Fig. 9. As is shown in Fig. 9, 7×7 is the most stable phase for the positive chemical potential up to $\mu = 0.1145$ eV, where 9×9 and 7×7 phases have the same free energy. The structure of the 7×7 phase is stable for the chemical potential in a wide range, which must be the reason for the high amount of the 7×7 phase observed in Fig. 4.

There exist 5×5 and 11×11 phases in Fig. 4, but they are only in the form of the half-SF cells. Concerning the 5×5 phase, since the atomic density is considered to be higher on the surface prepared by quenching, the 5×5 phase must be less stable in this condition, which is in good agreement with the observed results. In fact, as shown in Fig. 9, 7×7 is the most stable phase even in the negative region of the chemical potential
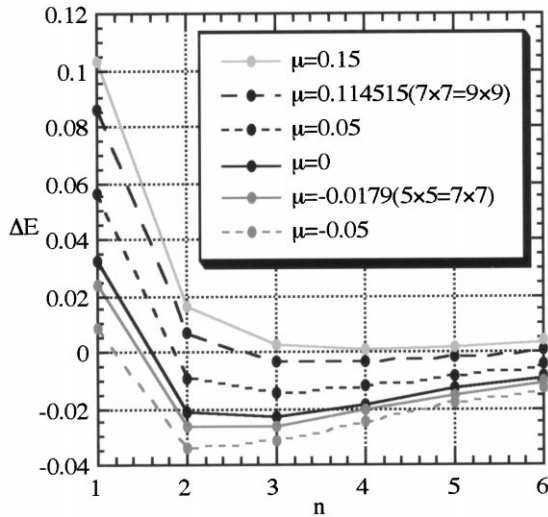

Fig. 9. Change in the relative structural energy of $\Delta E(n)$ [Eq. (1)] with the value of the chemical potential.

down to $\mu = -0.0179$ eV, where 5×5 and 7×7 phases now have the same free energy. Therefore, existence of the 5×5 SF half-cells may be due to the fluctuation in the local atomic density during quenching. On the other hand, the 11×11 phase is essentially not stable, as shown in Fig. 9, which is consistent with the observed result. In fact, the large DAS domains grown on a quenched surface observed by Yang and Williams [23] and Ohdomari and coworkers [11] was up to the 9×9 phase.

As is shown here, the observed result is consistent with the mechanism introduced by Yang and Williams, and Vanderbilt [15,23]. Excess atoms are produced during the phase transition from the higher atomic density '1×1' phase to the 7×7 phase, and remain on the surface by quenching instead of being incorporated at the step edges, which induces the formation of the higher atomic density phase. In fact, excess Si atoms are scattered in the disordered area on the surface, as shown in Fig. 4a. However, since the energy balance analyzed in this model is related to the units of the $(2n+1) \times (2n+1)$ DAS structures, its prediction is still limited to the comparison in a static form. Therefore, in order to understand the role of the completed corner hole in more detail, it is necessary to understand the stability of the DAS structure at a subunit level. Let us discuss the model shown in Fig. 8 further.

3.3. Energetic analysis of the DAS formation process at a subunit level

Fig. 10 shows the schematic model for the formation of one 7×7 SF half-cell. Several formation paths are possible at the atomic level. Then, in order to estimate the structural energies, discussion here is limited to the $(2n+1) \times (2n+1)$ SF structures: (a) 3×3 (completed corner hole), (b) 5×5, (c) 7×7, (d) $7 \times 7 +$ dimer, (e) $7 \times 7 +$ corner hole without SF, and (f) completed 7×7 SF unit. From the experimental results, the $(2n+1) \times (2n+1)$ DAS structure grows from a completed corner hole to form a 7×7 SF structure (Fig. 10a–c), and dimers are formed on the other side in Fig. 10d.
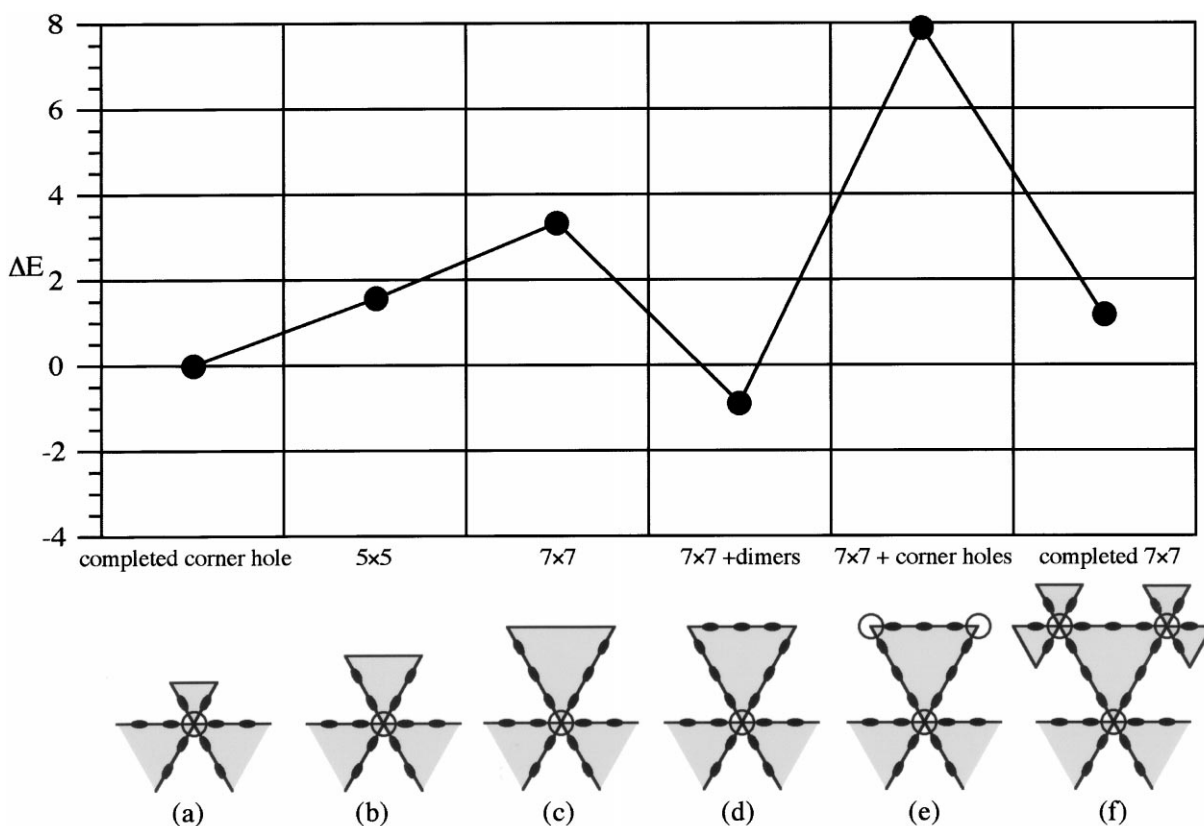
Fig. 10. Schematic of the formation of 7×7 SF half-cell. The change in the relative structural energy is also shown.

The 7×7 structure is formed completely by the formation of the corner holes that exist on the other end of the SF unit (Fig. 10f). Relative structural energies corresponding to the schematics in Fig. 10 were estimated using the values of Δf, p (dangling bond energy), d (contribution per dimer to the surface energy), and c (contribution per corner hole to the surface energy) that Vanderbilt adopted to obtain the Eq. (1) [14]. As is shown in Fig. 10, growth of the fractional SF structures increases the energy, and the 7×7 SF cell is stabilized by the formation of the dimers on the other end of the SF cell. The observed structures in Fig. 6 are quite consistent with this model. A similar analysis including the effect of oxygen was recently carried out by Hoshino et al. using the extended Hückel method on the cluster model [26]. Their analysis can be compared with the change in Fig. 10a–d. The general characteristic of

the energy diagram, which mainly depends on the number of dangling bonds, is quite consistent between the two cases. The existence of oxygen lowers the structural energy, but since the general characteristic is similar, we treat the oxygen-free structure here.

For further growth of the 7×7 phase on the surface, corner holes must be formed on the other end of the newly formed SF cell (Fig. 10e). When an apparent corner hole without an SF structure is formed on the surface the structural energy increases as $c+p=4.16$ eV for each one (Fig. 10e), which is considered to be a possible barrier height in the process of the formation of the completed corner hole; see Fig. 10d–f. As is shown in Fig. 10, there exist two barrier heights for the growth of 7×7 structure: the formation of the SF cell (from Fig. 10a–d), and the formation of the completed corner holes (from Fig. 10d–f). Since the barrier

height in the latter is higher, the formation of the completed corner hole may work effectively as the rate-limiting process in this model. In fact, as described above, during the annealing of the quenched surface, the growth and annihilation of single $(2n+1)\times(2n+1)$ SF cells (Fig. 10a to c or d) were observed to occur. After the structure of the corner hole is completed on the other end of the SF cell (Fig. 10f), growth of the SF cells is followed sharing the corner holes, which is also in good agreement with the observed results. Since the activation energy for the formation of the completed corner hole (Fig. 10d–f) seems to be high, the oxygen-related process proposed by Ohdomari and coworkers may play some role in reducing the barrier height [18,26].

As has been shown, the results obtained look quite consistent. However, if the formation of the completed corner hole is the only limiting process, SF cells can be formed from a corner hole of an SF cell into two symmetric directions. This still does not explain the triangular shape of the $(2n+1)\times(2n+1)$ DAS domain growth with successive additions of single SF half-cells. Therefore, there must exist some other factor in the domain growth process. Let us examine the remaining problem next.

3.4. Phase matching in the formation process

When formation of the completed corner hole is the rate-limiting process, phase matching of the SF units strongly affects the formation process of the DAS structure. Namely, when different sizes of DAS structures are formed from the same corner hole, the domain growth of a single phase DAS structure must be hampered by the phase mismatching, which is considered to govern the growth velocity of the DAS domains. From this standpoint, let us examine the formation process of the DAS domain in detail.

3.4.1. Characteristic structure of the boundaries between the DAS and disordered areas

An STM image obtained over a quenched surface is shown in Fig. 11a. Here, we chose the area which has a zigzag boundary consisting of SF half-units for the analysis of the growth process.
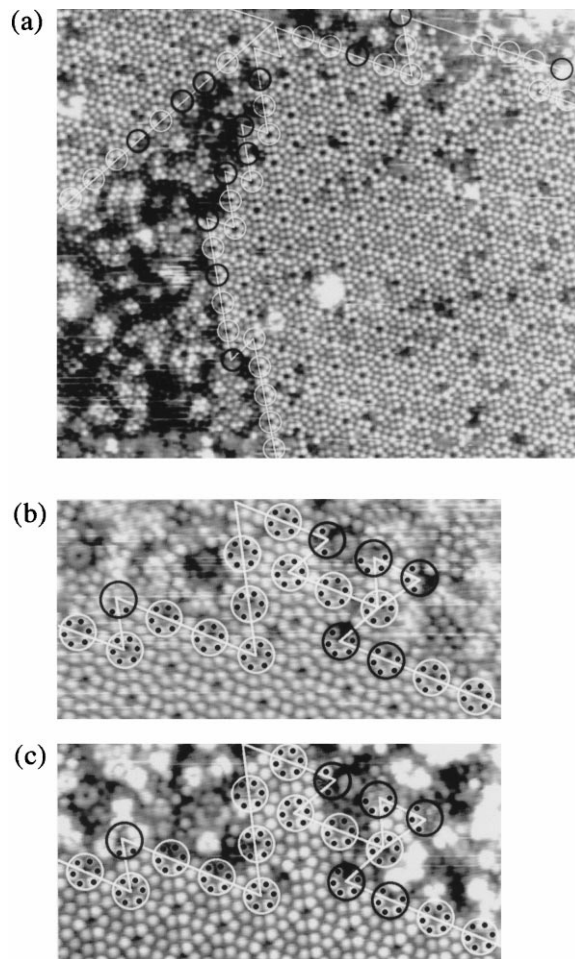

Fig. 11. (a) STM image of a quenched Si(111) surface ($V_s = -2.0$ V, $I_t = 0.3$ nA). Characteristic structure of the boundary with (b) positive ($V_s = 2.0$ V, $I_t = 0.3$ nA) and (c) negative ($V_s = -0.5$V, $I_t = 0.3$nA) bias voltages. Corner holes at the boundary with complete and incomplete structures are indicated by white and black circles respectively.

Fig. 11b and c show the empty-state ($V_s = 2.0$ V, $I_t = 0.3$ nA) and filled-state ($V_s = -0.5$ V, $I_t = 0.3$ nA) STM images of a characteristic zigzag structure at the boundary between the 7×7 and disordered structural areas. From comparison between Fig. 11b and c, it is clear that the structure of corner holes and dimer chains are formed along the straight domain boundaries, as expected. On the other hand, the structure of corner holes is not completed at the kink sites; triangular edges of the 7×7 structural area formed in the disordered area.

Namely, growth of 7×7 domain is considered to be suppressed at the edges. In Fig. 11, corner holes at the boundary with complete and incomplete structures are indicated by white and black circles respectively. When the structure of a corner hole is completed at an edge of the boundary, another SF cell of the DAS structure must be formed to reproduce the observed structure. The observed result also supports the model that the formation of the completed corner hole is the rate-limiting process in the growth of the DAS structure.

3.4.2. P- and S-processes in the formation mechanism

A schematic of the boundary structure is shown in Fig. 12a. From the edge of the SF unit indicated by E in Fig. 12a, there are two possible processes for an SF cell to be formed; an SF unit can grow in the directions parallel or perpendicular to the domain boundary, as shown in Fig. 12b by the arrows P and S respectively. We term these two processes P- and S-processes respectively. According to high temperature STM studies, the 7×7 domain grows by forming SF cells along domain boundaries between the 7×7 and disordered structural areas, instead of perpendicular to the boundary [13], corresponding to the P-process.

Let us compare the two formation processes of an SF unit more in detail. Fig. 13 schematically shows the recombination progress of each Si-bond
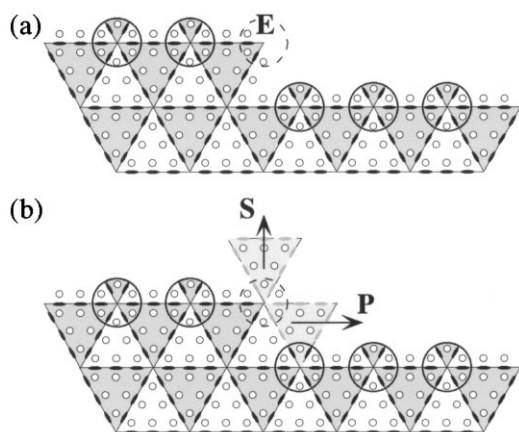

Fig. 12. (a) Schematic of the boundary structure in Fig. 11. E indicates an edge of the SF unit in the domain. (b) Two possible growth processes for an SF unit from the edge E in (a).

in the formation of an SF cell by the P- and S-processes. In any case, a DAS structure is formed from a completed corner hole and is stabilized by the formation of the dimers that exist on the other end of the SF cell, as shown in Fig. 10d. For further growth, corner holes must be completed as shown in Fig. 10f. In the case of the P-process, since two of three corner hole positions are fixed from the beginning, the formation of the SF cell is performed easily. On the other hand, in the case of the S-process, since the SF unit begins to grow from one corner hole, there exists an uncertainty for the positions of the another end of the SF cell. The uncertainty has already been observed in the case of the DAS fragment formation in a disordered area shown in Fig. 6. When DAS structures with different sizes are formed sharing the same corner hole, they must change so that their sizes become the same for the growth of the structural domain consisting of a single size DAS structure. In addition, the dangling bond energy of 1.45 eV dominantly affects the change in the energy during the formation process, and the number of dangling bonds appearing in the process is larger for the S-process, as shown in Fig. 13c. In the more detailed energetic analysis by Hoshino et al., the P-process-like formation was concluded to be the most probable path [26]. For the reasons shown here, an SF unit must be formed in the P-process more easily than in the S-process. This fact causes the preferential growth of the DAS structural domains along the domain boundary, resulting in the growth of the domains with a rather straight domain boundary. Once a straight boundary is formed the structural energy is lowered, as shown in Fig. 10a. This process is quite consistent with the experimental result obtained by Ohdomari and coworkers [13]. As described above, a similar structure was observed in a breakdown process induced by HBO_2 irradiation; completed corner holes remain on the straight boundary between 7×7 and disordered phases [19]. Therefore, the stability of the completed corner hole is also working in the breakdown process of the DAS structure.

Let us examine again the structure where the 9×9 phase was formed in additional to the 7×7 domain during quenching (Fig. 7). When the
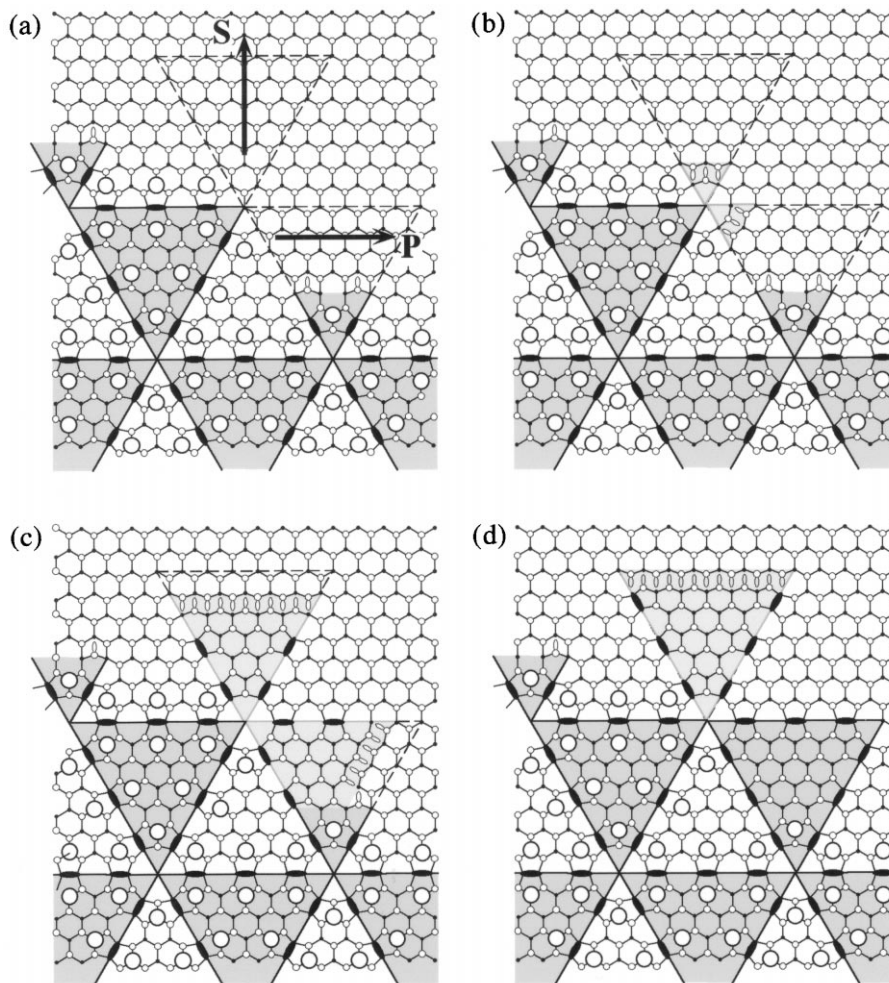
Fig. 13. A schematic of the recombination process of each Si-bond in the formation of an SF unit by the P- and S-processes shown in Fig. 12b.

corner holes on the boundary between the 7×7 triangular domain and the disordered areas are shared, the 9×9 domain growth must adopt the S-process in order for phase matching. In fact, the 9×9 domains are formed in the direction perpendicular to the boundary between the 7×7 and disordered areas, as shown in Fig. 7.

Since the 7×7 structure has already grown around the step edges even on the quenched surface, it is difficult to analyze the detailed formation process at the step edges here. However, the 7×7 structure may easily be formed at step edges by

the P-process in a similar fashion to that shown in Fig. 12.

4. Conclusion

By considering the charge transfer from adatoms to rest atoms, the structure of the dimer and stacking fault layers in the Si(111) DAS structure was analyzed at the subunit level on a quenched surface. A corner hole with a completed stacking fault and dimer structures in the second layer, i.e.

a completed corner hole, was confirmed to play an important role not only in the mechanism to stabilize the DAS phase, but also in the formation process of the DAS structure; the formation of the completed corner hole is the rate-limiting process for the growth of the DAS structure. The results obtained were shown to be quite consistent with the mechanism previously proposed by Yang and Williams [12] and Vanderbilt [15] on the basis of the effect of the excess atoms, i.e. the chemical potential for Si atoms in the surface layer. With this mechanism, the growth process of the DAS structure was explained comprehensively.

Acknowledgements

References

[1] K. Takayanagi, Y. Tanishiro, M. Takahashi, S. Takahashi, J. Vac. Sci. Technol. A: 3 (1985) 1502.
[2] G. Binnig, H. Rohrer, Ch. Gerber, E. Weibel, Phys. Rev. Lett. 50 (1983) 100.
[3] R.M. Tromp, R.J. Hamers, J.E. Demuth, Phys. Rev. B 34 (1986) 1188.
[4] C.B. Duke, Chem. Rev. 96 (1996) 1237.
[5] R.J. Hamers, Y. Wang, Chem. Rev. 96 (1996) 1261.
[6] S. Kitamura, T. Sato, M. Iwatsuki, Nature 351 (1991) 215.
[7] K. Miki, Y. Morita, H. Tokumoto, T. Sato, M. Iwatsuki, M. Suzuki, T. Fukuda, Ultramicroscopy 42–44 (1992) 851.
[8] R.S. Becker, J.A. Golovchenko, G.S. Higashi, B.S. Swartzentruber, Phys. Rev. Lett. 57 (1986) 1020.
[9] M. Tomitori, F. Katsuki, O. Nishikawa, J. Microscopy 152 (1988) 337.
[10] M. Tomitori, F. Iwawaki, N. Hirano, F. Katsuki, O. Nishikawa, J. Vac. Sci. Technol. A: 8 (1990) 222.
[11] T. Hoshino, K. Kokubun, K. Kumamoto, T. Ishimaru, I. Ohdomari, Jpn. J. Appl. Phys. 34 (1995) 3346.
[12] Y.-N. Yang, E.D. Williams, Phys. Rev. Lett. 72 (1994) 1862.
[13] K. Kumamoto, T. Hoshino, K. Kokubun, T. Ishimaru, I. Ohdomari, Phys. Rev. B 53 (1996) 12 907.
[14] D. Vanderbilt, Phys. Rev. B 36 (1987) 6209.
[15] D. Vanderbilt, Scanning Microsc. 8 (1996) 794.
[16] M.C. Payne, J. Phys. C: 20 (1987) L983.
[17] K. Kumamoto, T. Hoshino, K. Kokubun, T. Ishimaru, I. Ohdomari, Phys. Rev. B 52 (1995) 10 784.
[18] I. Ohdomari, Surf. Sci. 271 (1992) 170.
[19] K. Miyake, M. Ishida, K. Hata, H. Shigekawa, Phys. Rev. B 55 (1997) 5360.
[20] K. Miyake, H. Shigekawa, R. Yoshizaki, Appl. Phys. Lett. 66 (1995) 3468.
[21] K. Miyake, M. Ishida, M. Uchikawa, K. Hata, H. Shigekawa, Y. Nannichi, R. Yoshizaki, Surf. Sci. 357–358 (1996) 464.
[22] T. Hoshino, K. Kumamoto, K. Kokubun, T. Ishimaru, I. Ohdomari, Phys. Rev. B 51 (1995) 14 594.
[23] Y.-N. Yang, E.D. Williams, Scanning Microsc. 8 (1996) 781.
[24] R. Wolkow, Ph. Avouris, Phys. Rev. Lett. 60 (1988) 1049.
[25] Ph. Avouris, R. Wolkow, Phys. Rev. B 39 (1989) 5091.
[26] T. Hoshino, N. Kamijou, H. Fujiwara, T. Watanabe, I. Ohdomari, Surf. Sci. 394 (1997) 119.